*Korean J. Chem. Eng.*, 34(6), 1846-1857 (2017)
DOI: 10.1007/s11814-017-0084-3

pISSN: 0256-1115
eISSN: 1975-7220

# Propagation speed of wrinkled premixed flames within stoichiometric hydrogen-air mixtures under standard temperature and pressure

**Zuo-Yu Sun† and Guo-Xiu Li†**

School of Mechanical, Electronic and Control Engineering, Beijing Jiaotong University, Beijing 100044, China
(*Received 12 July 2016 • accepted 20 March 2017*)

**Abstract**—To explore the influence mechanism of initial turbulence on propagation speed of wrinkled flames, the turbulent combustion behavior of wrinkled stoichiometric hydrogen premixed flames was studied in a spherical fan-stirred closed vessel under standard temperature and pressure. The variations on flame structure were first observed; turbulent flames first were distorted and then became cellular, and both first and second critical flame radii of cellularity declined with a increased rate as turbulent intensity rose. Then, the variations of stretch effects were compared to laminar flame; the global stretch rate on turbulent flame at a same flame size was raised while the enhancement extent was obviously enlarged with the increase of initial turbulent intensity and/or the growth of flame size. Finally, the variation regulations of propagation speed induced by varying turbulent intensity were analyzed; the nexus between propagation speed and initial turbulence was discussed with the considerations of cellularity phenomenon and stretch effects.

Keywords: Cellularity Phenomenon, Hydrogen Premixed Flame, Stretch Effects, Turbulent Flame Speed, Wrinkled Flame

## INTRODUCTION

To the Far East region, which has fallen into energy shortages and environmental deterioration, hydrogen gas has been widely regarded as one utmost promising alternative energy source for its high calorific value, abundant supply reserves, and clean combustion products [1-4]. During the past two decades, hydrogen gas as the fuel has been tested in various energy conversion systems (including internal combustion engines, gas turbines, power plants, etc.) within most Far East countries (such as China, India, Japan, Korea, Malaysia, Russia, etc.) [5-10]. Albeit brilliant performance has been gained in those prototypes, the industrial application of hydrogen-fuelled power devices has still a long way to go, since an enormous number of scientific issues about hydrogen's combustion process need to be solved. Therefore, relevant studies about hydrogen's fundamental combustion characteristics are always hot topics in the field of energy science and chemical engineering [11].

Turbulent premixed combustion is the conventional combustion mode in practical thermal engines, and wrinkled flamelets [12] is the conventional regime into which most turbulent premixed flames belong; and thus, wrinkled premixed flames are often taken as the studied objects. Turbulent propagation speed ($u_{tr}$) is one key parameter linking most scientific issues about turbulent combustion (such as directly assessing actual combustion process [13], accurately predicting combustion performance [14], auxiliary validating chemical reaction mechanism [15], and so on), and hence the related studies on $u_{tr}$ of wrinkled premixed flames are widely of concern to scholars. However, most previous studies have been conducted on hydrocarbon fuels [16-20] rather than hydrogen gas; related experimental data thus are scarce from hydrogen flames in the current. From the literature [21-25], it could be known that, under standard pressure and temperature, most hydrocarbon premixed flames are stable and smooth, but hydrogen premixed flame (especially lean and stoichiometric mixture) is always cellular and unstable due to its fierce inherent instabilities, and the inherent instabilities could bring remarkable effects on flame propagation speed especially enters into the period of 'self-tubulisation'; therefore, hydrogen flame gives obvious differences on the aspects of inherent instabilities and the detailed nexus to propagation speed. However, many current combustion models, such as turbulent combustion models about burning velocities [26], blast wave predication models [27], and turbulent combustion models about instabilities [28]) were mainly established upon the experimental data from hydrocarbon fuels, and hence there exists incomplete applicability of those models on hydrogen flames. Since flame speed is essential and crucial to validate the prediction accuracy of combustion model, obtaining turbulent propagation speed of hydrogen premixed flames and discussing the influence mechanism of initial turbulence on propagation speed are still necessary no matter for correct current models or establishing novel model(s) for hydrogen.

For providing more insight into hydrogen premixed flames' turbulent combustion characteristics, the present investigation takes wrinkled stoichiometric hydrogen-air premixed flames as flame samples, observes the effects of initial turbulent flow on hydrogen premixed flames' detailed evolution process, measures experimental values of turbulent flame speed, and analyzes the nexus between turbulent flame speed and flame's cellularity phenomenon.

†To whom correspondence should be addressed.
E-mail: sunzy@bjtu.edu.cn, li_guoxiu@yahoo.com
‡The paper will be reported in the 11th China-Korea Clean Energy Workshop.

## EXPERIMENTS AND METHODS

### 1. Method of Experiment

The reported experiments were carried out in a single-layer, constant-volume, fan-stirred closed combustion vessel. The vessel was designed into a spherical cavity (inner diameter: 380 mm; net volume: 28.73 L). Upon the vessel, four quartz windows (effective diameter: 120 mm; thickness: of 30 mm) were orthogonally mounted to provide optical access, four fans (each fan has five tetrahedron blades and one central mounting hole; in tetrahedron gross diameter of fan: 90 mm; width of blade: 15 mm; diameter of mounting hole: 14 mm) were mounted in pyramidal configuration (whose geometric center is located in the vessel's center), and one pair of electrodes (tungsten material; diameter: 2.5 mm; mounting gap: 2 mm) was mounted to ignite combustible mixture at the vessel's center. Each fan was respectively coupled to an independent electric motor via the magnetic to avoid leakage; ahead each fan, one piece of circular porous plate (gross diameter: 110 mm; diameter of hole: 12 mm; number of hole: 37; distance between two neighboring holes: 3 mm) was mounted to transfer the swirl flow induced by fan's rotation into jet flows. Such jet flows from multiple directions run into the collision at the vessel's center to generate a fierce turbulence; the turbulent intensity could be changed by adjusting fan speed and/or changing porous plates into different structures. Images of practical vessel, practical fan, practical porous plate and the schematic of turbulence generation are demonstrated in Fig. 1.

Schlieren system (Z-arranged; focal length: 2,000 mm) was used as the optical access system, high-speed camera (FASTCAM SA-X2; operation rate: 13,500 frames per second; resolution: 1024×1000 pixels) was used to capture the development process of flame. A transient piezoelectric pressure transducer (Kistler 6052C) linked with a charge amplifier (Kistler 5018B) was used to monitor the pressure near the inner wall of vessel. A synchronous control unit was used to synchronously trigger the operation of ignition system, camera and pressure transducer.

Procedurally, the vessel was first evacuated into vacuum condition (actually, in the present investigation, it was evacuated down to 0.003 MPa), then it was respectively filled by hydrogen and air to the standard ambient pressure (0.100 MPa) according to Dalton's law of partial pressure. Once the mixture was prepared in the vessel, four fans were synchronously trigged and rotated with the same speed. After three minutes (to maintain turbulence '*steady*'), the ignition system, the high-speed camera system, and the data acquisition were synchronously triggered to realize the ignition and the capture of related information. After one set of experiments, the vessel was flushed (three times) with air to remove residuals, and then it was again evacuated to the vacuum condition for the next experiment.

In the present investigation, six sets of fan speed were used to generate six different cases of turbulence (including laminar condition), the corresponding relationship between fan speed and turbulent intensity is listed in Table 1. The hydrogen was pure hydrogen gas with a purity of 99.999%, and the air was synthetic air (mixed by pure oxygen gas and pure nitrogen gas in a volume ratio of 21:79).

### 2. Definition of Parameters

Flame propagation speed ($u_l$ and/or $u_{tr}$) is always defined as the normal extension rate of flame-front within combustion process, and thus it is depending on the measurement of flame-front's size. For a laminar premixed flame, flame-front's size (always indicated by flame radius) could be easily derived from its smooth spherical

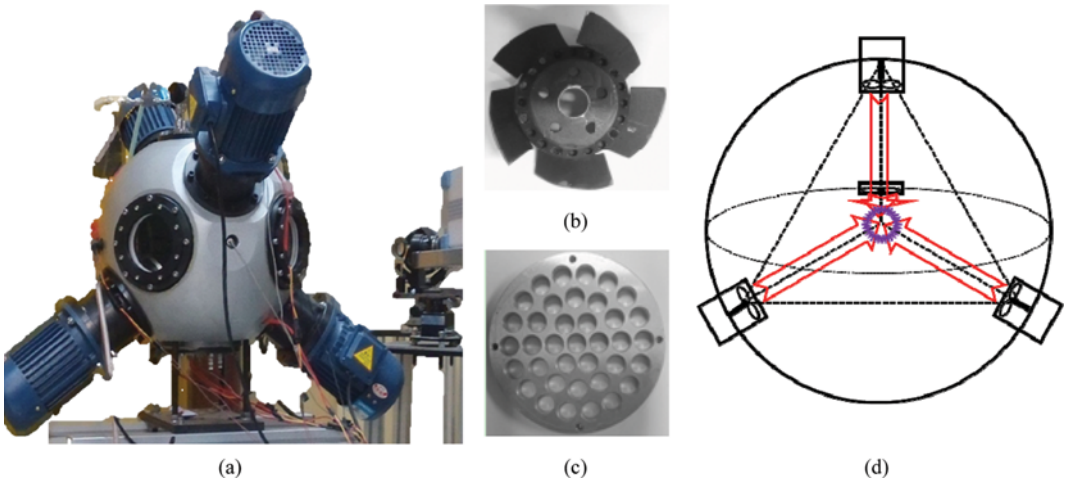


**Fig. 1. Schematic representation of (a) practical vessel; (b) practical fan; (c) practical porous plate; and (d) turbulence generation.**

**Table 1. Corresponding relationship between turbulent intensity and fan speed in the present investigation**

| Parameter | Case 1 | Case 2 | Case 3 | Case 4 | Case 5 | Case 6 |
|---|---|---|---|---|---|---|
| Fan speed (rpm) | 0 | 1136 | 1704 | 2272 | 2840 | 3408 |
| Turbulent intensity* (m/s) | 0.000 | 0.202 | 0.494 | 0.742 | 1.080 | 1.309 |

*Turbulent intensity here is defined as the rms (Root Mean Square) turbulent fluctuating in the centre of vessel

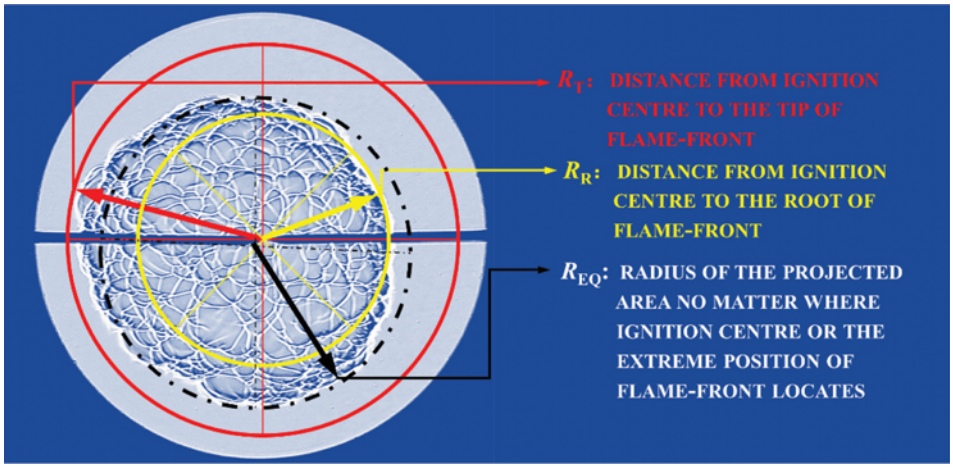


**Fig. 2. Schematic representation of a turbulent premixed flame's front.**

projected surface; however, the obvious flame brush makes such measurement certainly difficult on turbulent premixed flames [29, 30]. As shown in Fig. 2, either flame's root radius ($R_r$) or tip radius ($R_t$) is unsuitable to indicate flame front's size for the artificial reduction or increase on the projected area of flame-front. From previous scholars [31,32], equivalent radius ($R_{eq}$) of the projected surface area (A) was taken as the flame radius to determine turbulent flame propagation speed, as

$$u_{tr} = dR_{eq}/dt = d\sqrt{A/\pi}/dt = (1/\sqrt{\pi}) \times (d\sqrt{A}/dt) \quad (1)$$

Furthermore, for a better evaluation on the variation level of turbulent flame speed to laminar flame speed, normalized flame propagation speed ($u_{norm}$) was also used and defined as the ratio of $u_{tr}$ to $u_l$.

During the development process, the flame-front is always suffering the stretch effect from ambient mixtures, and the evolution of stretch effect is even an utmost influencing factor on the self-wrinkled phenomenon of laminar hydrogen premixed flames [33, 34]. Since the behavior of wrinkled turbulent premixed flames is similar to self-wrinkled laminar premixed flames [35], the evolution of stretch effect is valuable to be considered and analyzed. Learned from laminar premixed flames, global stretch rate ($\alpha$) was taken to assess the stretch effect and it is defined as the Lagrangian time derivative of the logarithm of the area of any infinitesimal element of the flame front as [36]

$$\alpha = d(\ln A)/dt \quad (2)$$

## 3. Repeatability of Results

Fig. 3 shows the observed development process of turbulent stoichiometric hydrogen premixed flames from five sets of experiments in the condition of $u'_{rms}$=1.309 m/s, namely, they came from five sets of '*Repeatability Test*'. As can be seen, even in the same condition, the detailed structures of turbulent hydrogen flames were still different, which means a turbulent premixed combustion process hardly could be '*absolutely*' repeated. However, during the development process, the onset of cellularity seemingly appeared at near flame size, while the evolution of flame also seemingly could be repeated.

For validating the '*Repeatability Test*' has repeatable sense in statistics, the evolution regulation of flame radius and the evolution of blast wave pressure were taken as the criteria [30]. Fig. 4 shows the comparison on the evolution of flame radius under the mentioned five sets of experiments; note that just the range of 7 mm to 50 mm has been adopted as reasonable for available flame radius. The criterion of 7 mm is from Bradley and co-workers [35,36] for avoiding the effects of ignition power, while the criterion of 50 mm is based upon the curve of blast pressure verse flame radius in the present investigation for avoiding the effects of reflected blast wave [37,38]. As can be seen from Fig. 4, within each set of experiments, $R_{eq}$ gave a similar growth tendency to time; most data could well match (albeit same data from Set I and Set III gave observed deviation at larger flame radius). Looking at the detailed variation of deviation to the average data, the relative deviation within each set falls into the range of ±5%; meanwhile, the relative deviation gave a coverage tendency in most sets rather than a monotonic rise.

Contingency tables analysis on the deviation of flame radius under the pointed range of time (from 0.4444 ms to 2.8148 ms with an interval of 0.0741 ms, which correspond to about 6 mm to 45 mm in $R_{eq}$), was made upon the obtained experimental results (5 sets multiply 33 number per set). The calculation results are in Table 2. The results indicate that the deviation of flame radius has no sense on either the time after ignition or the number of experiments.

Furthermore, 'the time to reach a blast wave pressure rise of 50%' was also taken as a criterion to assess the repeatability of turbulent combustion processes [15]. As can be seen in Fig. 5, the taken five sets gave a high similarity in the evolution of blast wave pressure, and the curves of pressures rise were also similar. In the details, all the obtained times to reach a blast wave pressure rise of 50% are around 5.642 ms with the ratio of range to average being no more than 2% (far less than 5%, the criteria to assess repeatability [15]), the variance is 0.003, Std. Var. (abbr. standard variance) is 0.050, and Coe. Var. (abbr. coefficient of variation) is 0.009. Upon the results, the turbulence combustion process could be regarded as repeatable. Since the combustion process could be regarded as repeatable in five sets of experiments, all the reported data were taken from the mathematically averaged values.

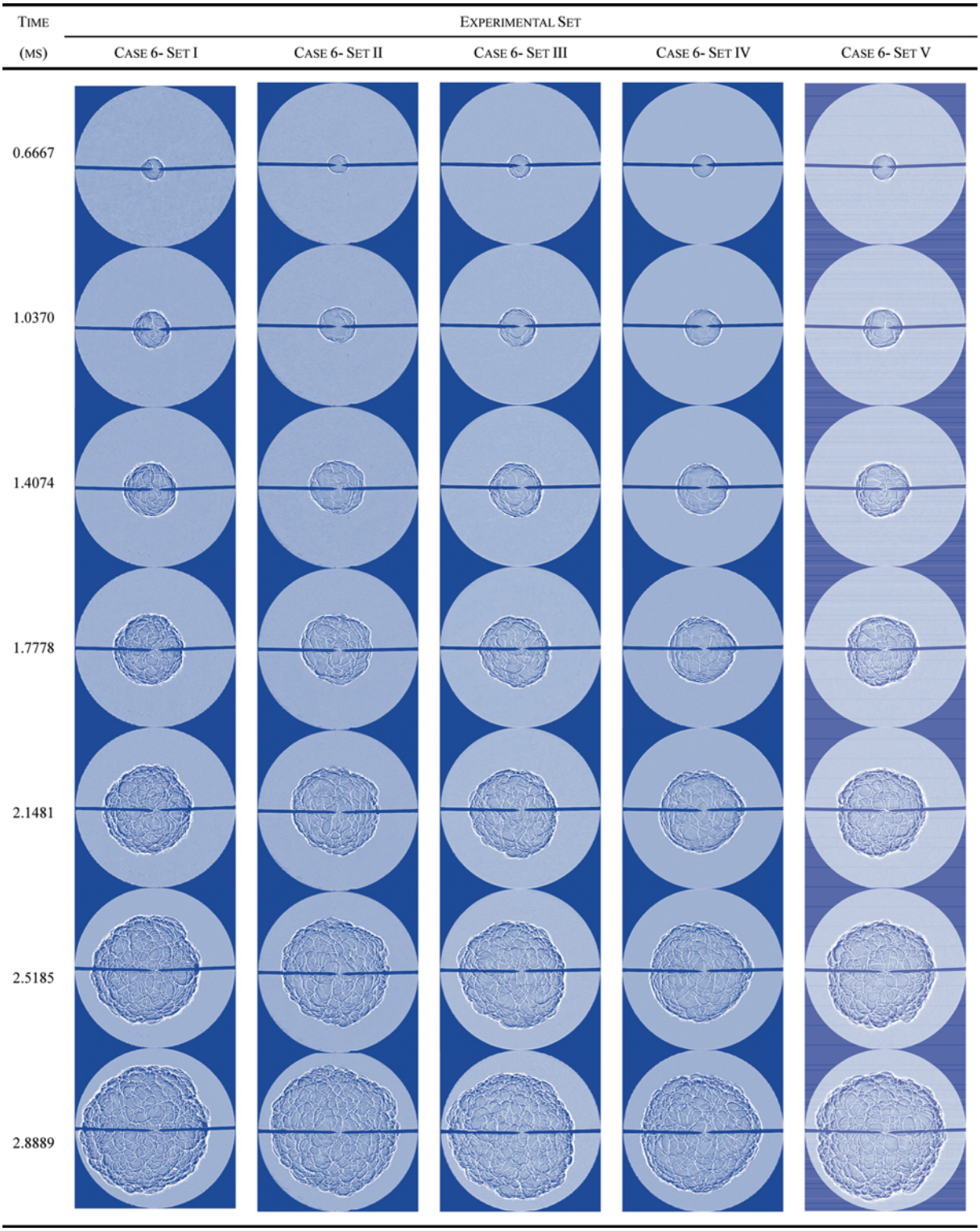


**Fig. 3. High-speed Schlieren imaging of stoichiometric hydrogen-air premixed flames propagating in the condition of $u'_{rms}$=1.309 m/s and STP.**

## RESULTS AND DISCUSSION

### 1. Cellularity Phenomenon

Fig. 6 shows the Schlieren images of stoichiometric hydrogen premixed flames as a function of time under different initial flow conditions. Under STP, no matter if it propagates in laminar ambience or turbulent ambience, the stoichiometric hydrogen premixed flame is always propagating towards the unstable from its initial

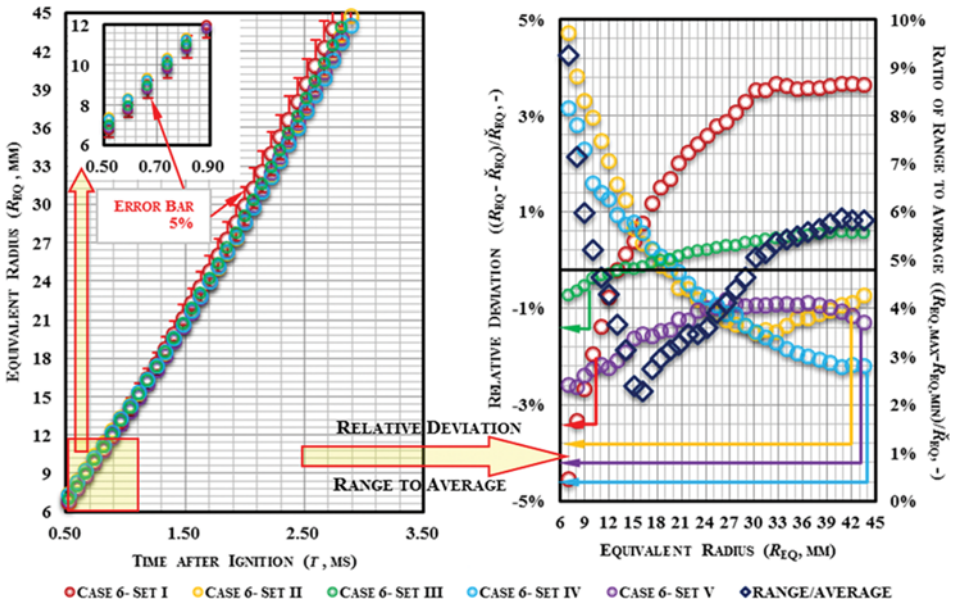


**Fig. 4. Comparison about repeatability on flame radius evolution in the cases of $u'_{rms}$=1.309 m/s and STP.**

**Table 2. Related results calculated by contingency tables analysis**

| Parameter | Chi-square probability | Chi-square statistic | Freedom | Confidence level | Critical value | Detection results |
|---|---|---|---|---|---|---|
| Results | 1.0000 | 17.0830 | 124 | 0.01 | 163.5465 | Accept the assumption Time after Ignition, and Test Times are not relevant |

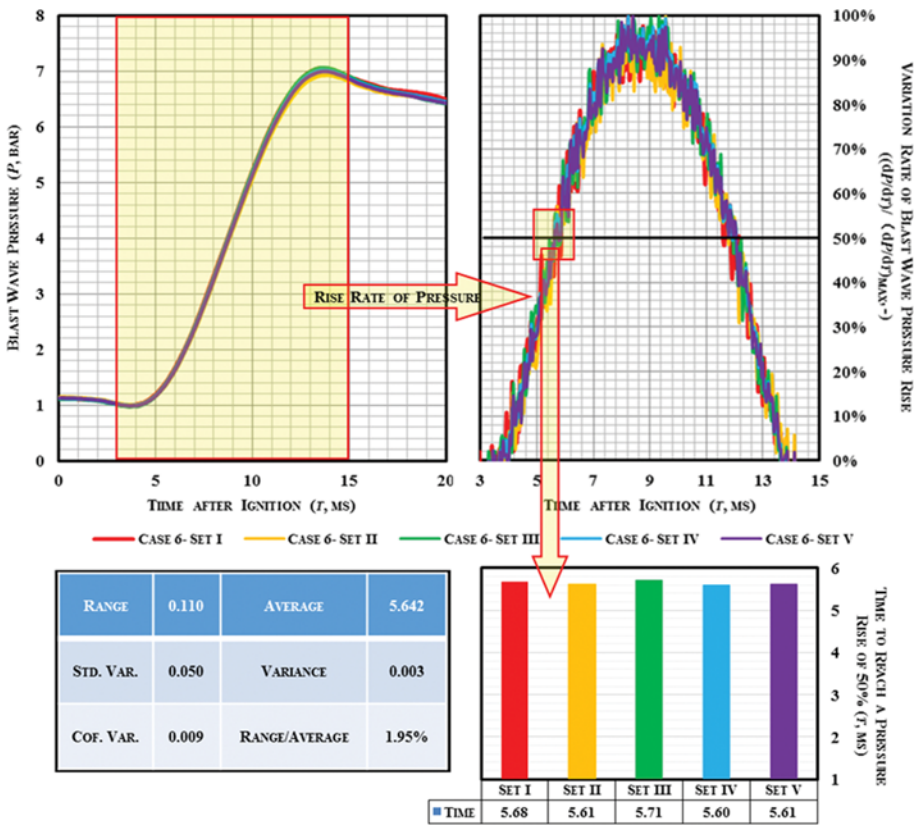


**Fig. 5. Comparison about repeatability on time to reach a pressure rise of 50% in the cases of $u'_{rms}$=1.309 m/s and STP.**

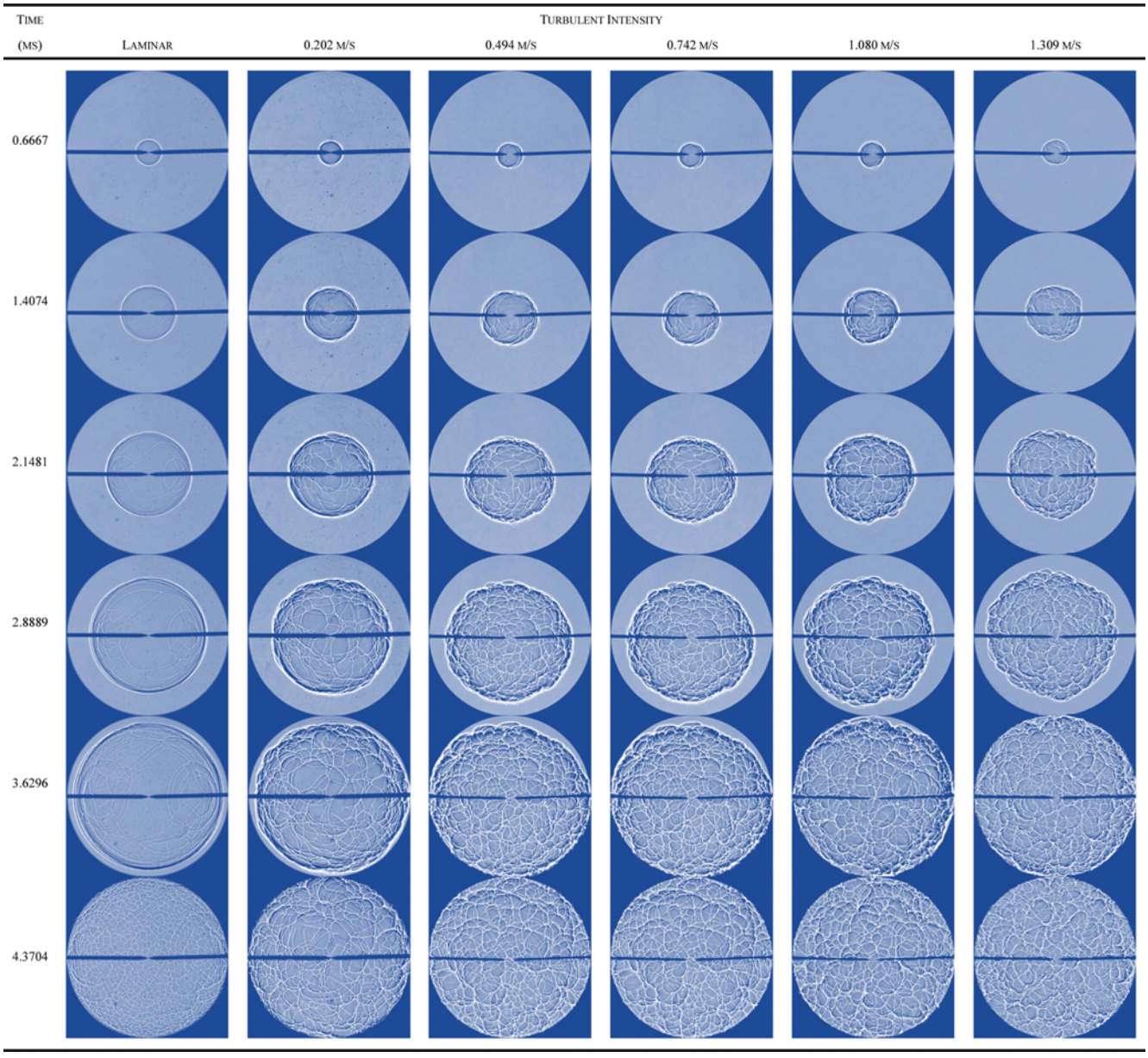


**Fig. 6. Turbulent premixed flames propagate in stoichiometric hydrogen-air mixtures with different initial turbulent ambience under STP.**

spherical and smooth shape.

Within laminar ambience, stoichiometric hydrogen premixed flame has an evolution in the stable; the flame front is always keeping the initial smoothness during the propagation process, although some cracks or even a few cells are formed on it. Within turbulent ambience, the appearance of stoichiometric turbulent hydrogen premixed flames in the initial period of propagation (such as the initial 0.5 ms) is very similar to laminar flame in both the shape of flame front and propagation speed; however, in the later period of propagation, turbulent flames are obviously wrinkled and the initial spherical shape won't be holed on. Meanwhile, numbers of cracks and cells fast and ceaselessly appear on the front to make flame noticeably cellular and unstable. With the increase of initial turbulent intensity ($u'_{rms}$), the time when flame front has been distorted is advanced, the level of such distortion is remarkably enhanced, the time when flame front has been entirely covered by cells is reduced, and the time when flame front has beyond the view field of window is shortened (namely, the propagation speed of flame is accelerated).

Based upon our previous investigations on laminar hydrogen premixed flames [32,39], hydrogen premixed flames have strong intrinsic instabilities which could make flame-front self-turbulent; and such self-turbulentization of stoichiometric hydrogen flame is attributed to its intrinsic hydrodynamic instability. In the present investigation, all the studied hydrogen flames were stoichiometric, namely hydrodynamic instability is the only existing intrinsic instability. From classic combustion theories, hydrodynamic instability is dependent on density ratio across flame-front and laminar flame thickness; the latter factor is a parameter relevant to laminar flame and has the same value for the same equivalence ratio in the pres-

ent investigation, which means it is not one influence factor to the variation for the present investigation. However, within turbulent ambience, all the physical parameters (including the densities of burned and unburned mixtures) fluctuate, and thus, the density ratio (the former factor determining hydrodynamic instability) could be changed and subsequently hydrodynamic instability varies.

From a finer point of view, it could be seen that, within the investigated experiments, the formation of cells is always after the distortion of flame-front, and thus, it could be regarded that ambient turbulence improves the probability of the appearance of cracks (in accordance with the characteristics of wrinkled flamelets), and subsequently promotes the formation of cells (in accordance with the regulation observed in laminar premixed flames). To quantitatively describe the regulation between turbulence and cellularity phenomenon, the first critical flame radius ($R_{cr,1st}$, which is defined as the flame radius at which initial cell has been formed [40]) and the second critical flame radius ($R_{cr,2nd}$, which is defined as the flame radius at which flame-front has been completely covered by cells [40]) of cellularity were employed. In Fig. 7, with the increase of turbulent intensity, both the critical flame radii of stoichiometric hydrogen premixed flames are monotonically reduced; meanwhile, the decline rates of both critical flame radii are gradually raised within the investigated range of ambient turbulence, which means that with a bit of increase in turbulent intensity, a larger enhancement in cellularity phenomenon could be attained.

As reported upon laminar premixed flames [32,39], the actual expansion area of flame-front would be increased by wrinkling even cellularity phenomenon, more unburned mixture subsequently would be strapped on flame-front to be burnt, and then propagation speed of flame would be correspondingly increased. Upon the above observed and analyzed, the higher the turbulent intensity is, the severer the cellularity phenomenon becomes, then the faster the propagation speed could be accelerated (as reflected in Fig. 6, demonstrated as the time flame-front beyond the view field

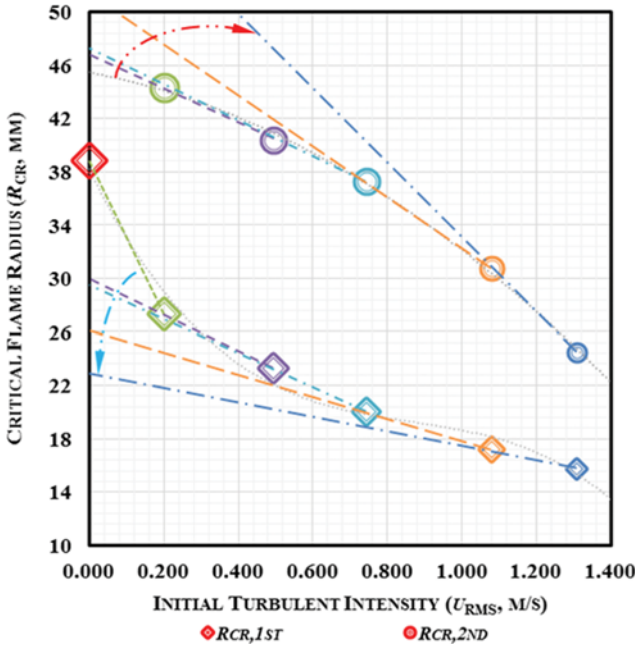


**Fig. 7. Critical flame radii of cellularity phenomenon of stoichiometric hydrogen premixed flames under different turbulent ambience.**

of window is advanced). More quantitative nexus about turbulent intensity and flame speed will be reported and discussed in the following subsection.

**2. Global Stretch Effects**

From classic combustion theories in laminar premixed flames, the global stretch effect plays an important role in the stabilization on flame front, and thus, analyzing the evolution of global stretch rate also could provide necessary evidence for the unstable development of turbulent premixed flames.

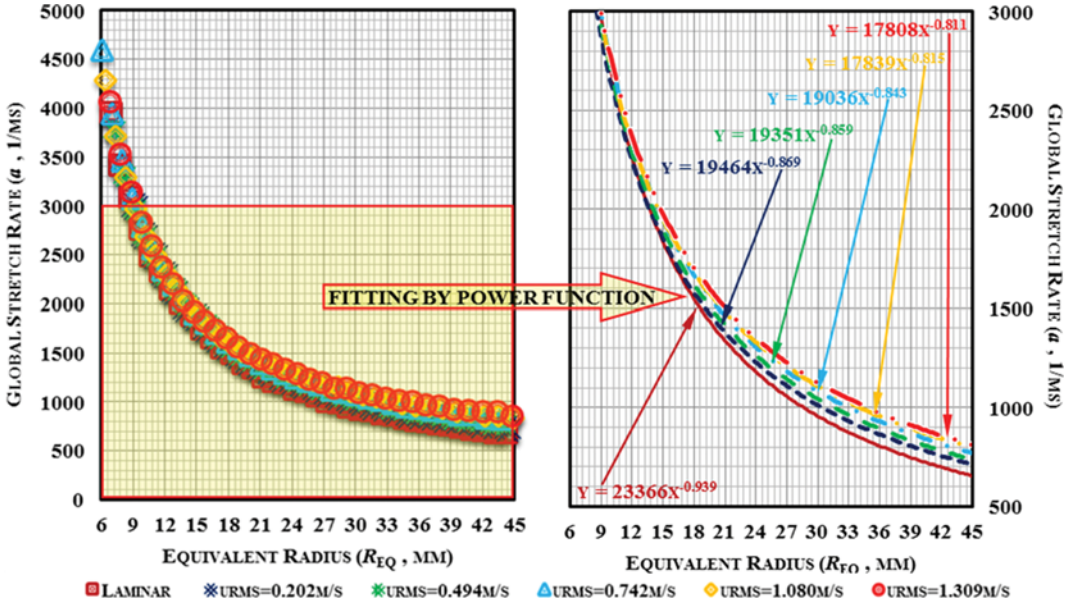


**Fig. 8. Evolution of global stretch rate of stoichiometric hydrogen premixed flames with different turbulent ambience under STP.**

Fig. 8 shows the evolution of global stretch rate of stoichiometric hydrogen premixed flames within different turbulent ambience. As can be seen, under each experimental condition, the global stretch rate of hydrogen premixed flames rapidly declines during the propagation process; at a specific flame size, the larger the turbulent intensity is, the higher the global stretch rate becomes, namely, the stronger the stretch effects on flame front becomes. Including the results obtained from laminar ambience, the monotonic decline of global stretch rate as the function of flame size exhibits nearly power tendencies. When the nexus of global stretch rate and flame radius has been fitted in a power function, with the increase of turbulent intensity, the empirical coefficient of $\alpha$-$R_{eq}$ function decreases, while the empirical power factor of $\alpha$-$R_{eq}$ function increases. Once the obtained data have been fitted, both the variation regulations of the empirical coefficient and the empirical power factor are nonlinear; moreover, the variation of such empirical constant gives a good coincidence once the absolute values of them are put into logarithm variations, as shown in Fig. 8. Such results mean that the effects of initial turbulence on global stretch effects are regular under certain mechanism rather than random.

For a better understanding the effects of initial turbulence on global stretch effects, the evolution of normalized global stretch rate

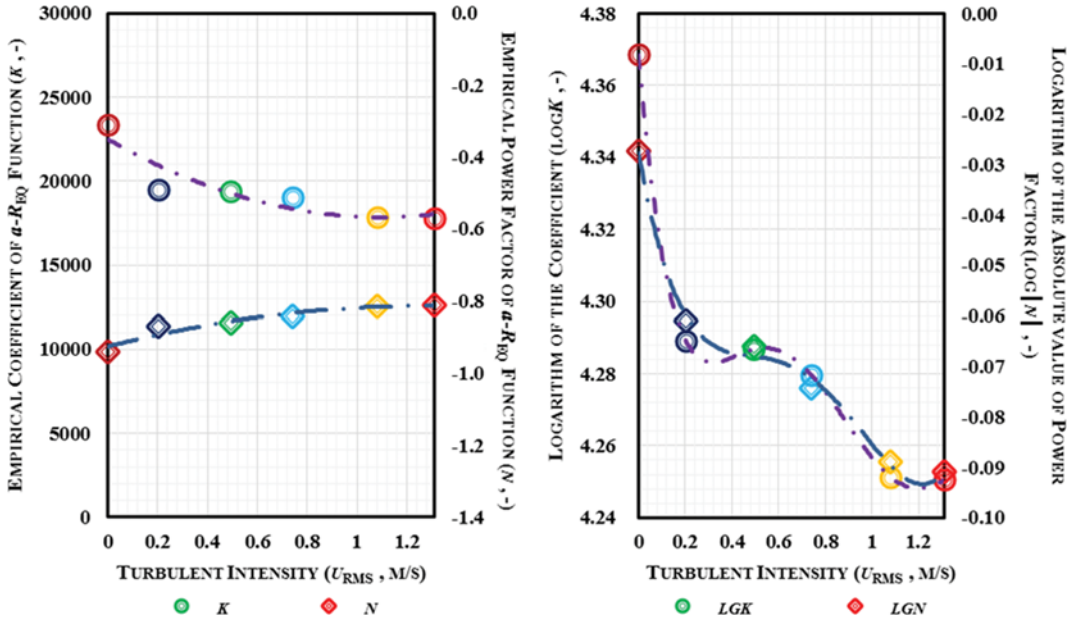


**Fig. 9. Nexus between empirical factors and initial turbulent intensities under STP.**

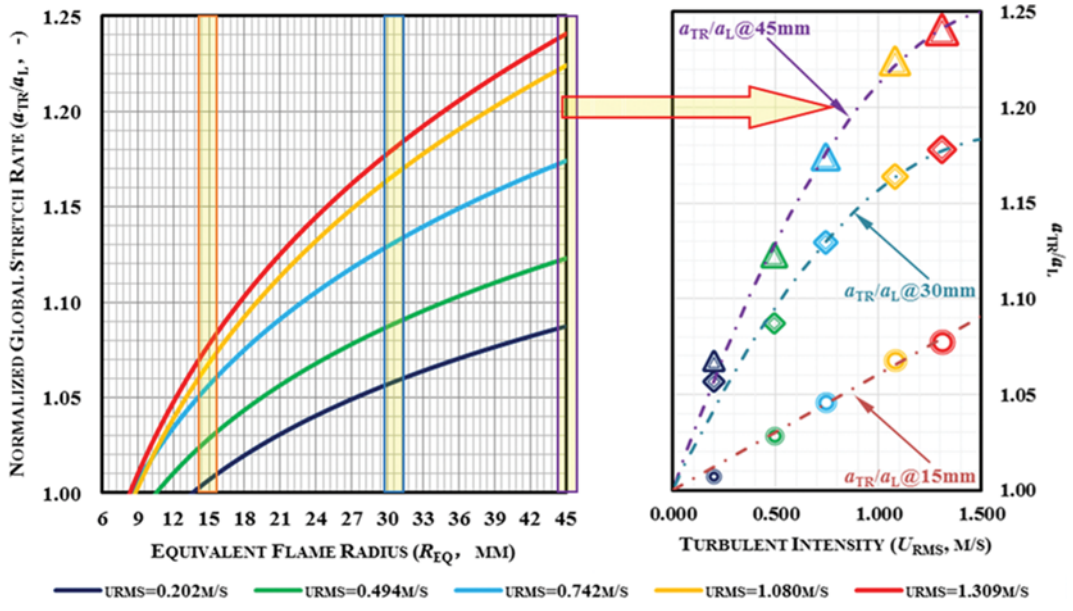


**Fig. 10. Evolution of the normalized global stretch rate versus the flame radius for stoichiometric hydrogen turbulent premixed flames under STP.**

($\alpha_{tr}/\alpha_l$, the ratio of global stretch rate on turbulent flame to global stretch rate on laminar flame with a same size) has been derived as shown in Fig. 10. The normalized global stretch rate monotonically rises with the development of stoichiometric hydrogen premixed flame, and the value of $\alpha_{tr}/\alpha_l$ at a same $R_{eq}$ generally rises with the increase of initial turbulent intensity. So two general conclusions can be drawn: (a) the influence of initial turbulence on the global stretch rate will continue to strengthen as flame develops rather than disappear; and (b) a stronger initial turbulence could have stronger influence on stretch effects. Global stretch effects are composed of two stretch factors for aerodynamic strain and flame curvature; flame curvature obviously is wrinkled as flame develops (as shown in Fig. 6) and this term is inevitably increased, while the ambient turbulence undoubtedly has positive effects on aerodynamic motion to, subsequently, the term of aerodynamic strain. Since the perturbation degree of turbulent premixed flames is more obvious than laminar premixed flames, and such disparity will be more and more serious as flame develops, it naturally results in the continuous increase in the term of flame curvature for stretch effects and correspondingly to the value of normalized global stretch rate.

Besides the mentioned macro trends, some interesting regulations also could be derived from the evolution of normalized global stretch rate. Together with the value of $\alpha_{tr}/\alpha_l$ at a specific $R_{eq}$=15 mm, such data could be well fitted in a linear tendency; when the viewport has been moved on $R_{eq}$=30 mm and/or $R_{eq}$=45 mm, order polynomial tendency seems more suitable to express the variation of such data as the function of initial turbulent intensity. Retrospective to the reported cellularity phenomenon, all the investigated flames show no sign of cellularity at $R_{eq}$=15 mm, but almost turbulent flames have been entirely cellular at $R_{eq}$=30 mm. From combining with cellularity phenomenon, it is reasonable to infer that (a) when flames Have not shown signs of cellularity, the global stretch effects are sufficiently strong (to suppress the appearance of instabilities as reported on laminar premixed flames [28]), and initial turbulent intensity has a stable effect on strengthening global stretch effects by influencing the term of aerodynamic strain; (b) when flame has been cellular, the global stretch effects have seriously declined and that hardly suppress instabilities any longer, and the share ratio of aerodynamic strain term would become weaker while the role of flame curvature term becomes more and more important, so the normalized global stretch rate still increase; and (c) although, the wrinkling flame curvature provides a positive role on the enhancement of global stretch effects, and the amplification would gradually be gentle for the sharply declining denominator.

### 3. Flame Propagation Speed

Still from the evolution of stretch effects, both the values of global stretch rate and the normalized global stretch rate are positive, which means the flame-front is suffering strengthening positively stretched rather than being compressed. Therefore, the flame propagation speed should be promoted by the existence of initial turbulence and such promotion would be continuously enhanced during combustion process.

Fig. 11 shows the evolution of flame propagation speed ($u_{tr}$) in stoichiometric hydrogen-air mixtures as a function of $R_{eq}$ with different turbulent intensities under STP. Under STP, the propagation speed of stoichiometric hydrogen premixed flames could be regarded as rising in a monotonic tendency during the period of constant-pressure combustion process, and the flame propagation speed at a specific $R_{eq}$ is raised with the increase of turbulent intensity. Generally, the growth tendency of laminar flame propagation speed could be regarded as linear for positive stretching, while the growth tendency of turbulent flame propagation speed seems more suitable for polynomial fitting. Given the information about cellularity phenomenon on the fitting plot of $u_{tr}$-$R_{eq}$, before the formation of initial cells on the flame-front (namely, the flame are still stable, shown as the zone below the blue line), the flame propagation speed linearly rises as flame develops; to the flames upon

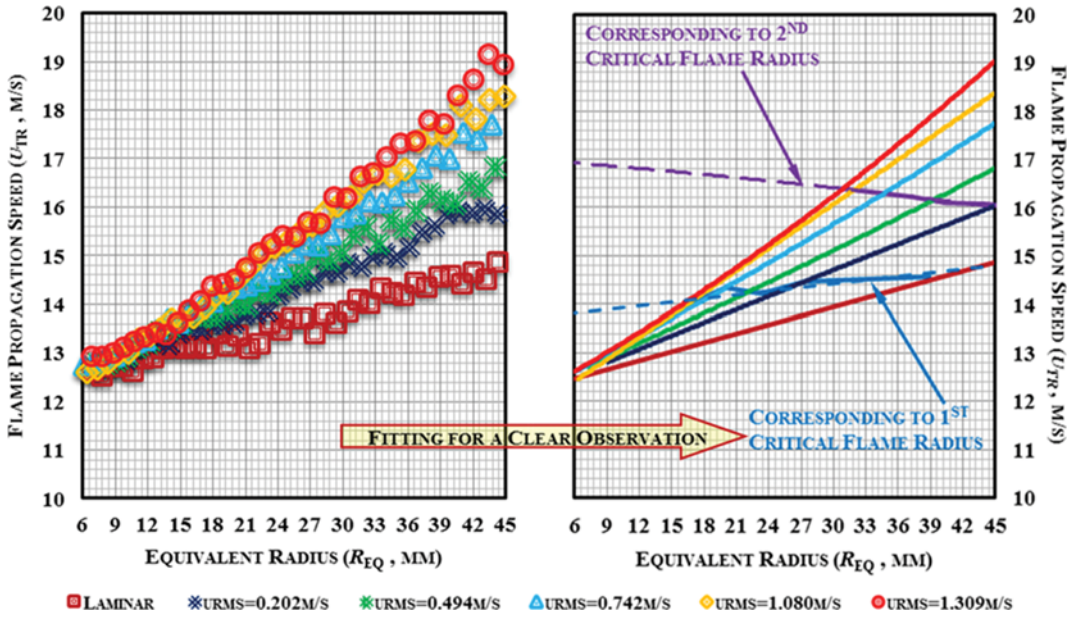


**Fig. 11. Evolution of turbulent flame speed in stoichiometric hydrogen-air mixtures with different turbulent intensities under STP.**

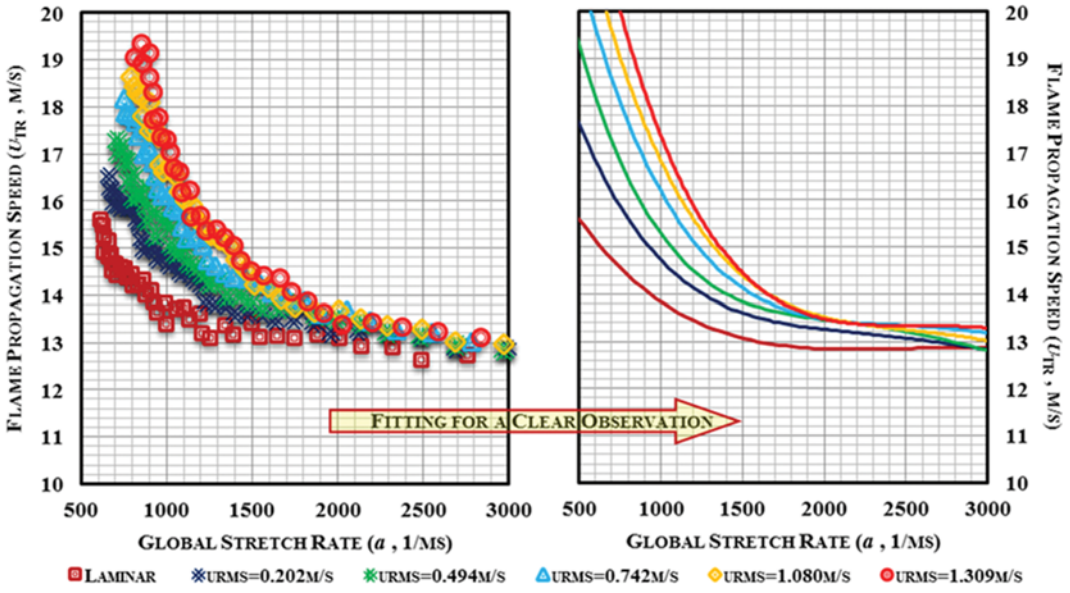


**Fig. 12. Evolution of flame speed in stoichiometric hydrogen-air mixtures as a function of stretch rate with different turbulent intensities under STP.**

whom cells are forming but have not entirely covered (shown as the zone between the blue line and the purple line), the flame propagation speed accelerating rises and such acceleration becomes more and more obvious with the increase of initial turbulent intensities. While, to the flames that have been entirely cellular (shown as the zone above the purple line), the flame propagation speed continues to accelerate and the acceleration is enlarged compared to the past period. Upon the observed phenomenon, the appearance and the development of cellularity phenomenon remarkably accelerates the flame propagation speed, and higher initial turbulent intensity has a more positive effect on such acceleration for the enhanced cellularity phenomenon.

Fig. 12 shows the evolution of flame propagation speed in stoichiometric hydrogen-air mixtures as a function of global stretch rate with different turbulent intensities under STP. To each investigated flame, the flame propagation speed generally rises in monotonic tendency with the decline of global stretch rate, but the concomitant variation of flame speed versus global stretch effects seems not active for the hydrogen premixed flame propagates in laminar ambient until the global stretch rate has declined to a certain value (such as 2000 1/ms). Compared to laminar premixed flame, turbulent premixed flame's propagation speed is higher at a specific

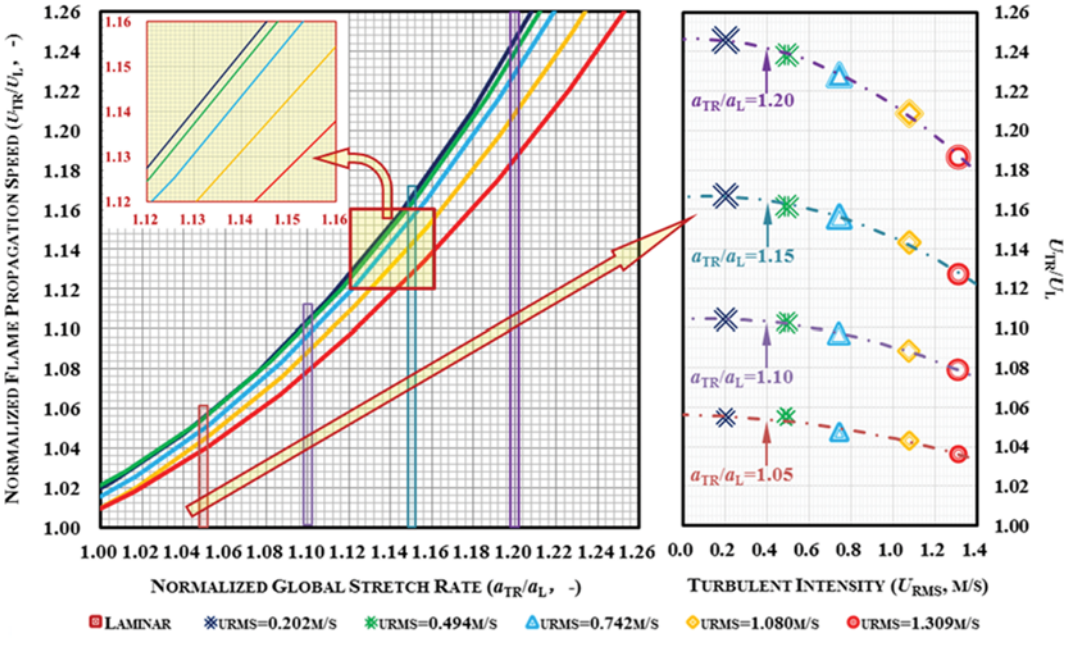


**Fig. 13. Nexus between normalized flame speed and normalized stretch rate of stoichiometric hydrogen premixed flame.**

$R_{eq}$; the increased extent is raised with the decline of global stretch rate and/or the increase of initial turbulent intensity.

Since global stretch rate also contains the influence of turbulence, a plot of normalized flame propagation speed and normalized global stretch rate could provide a clearer viewpoint for the further analysis. In Fig. 13, at each investigated initial turbulent ambience, with the increase of normalized stretch rate, the normalized flame speed monotonically rises; meanwhile, at each normalized stretch rate within the investigated range, the value of normal flame propagation speed is decreased with the increase of initial turbulent intensity (but such decline is not remarkable for the cases of $u_{rsm}$=0.202 m/s and 0.494 m/s). Furthermore, the detailed variations of normalized flame speed at four points of normalized stretch rate with an equal interval of 0.05 have been statistically compared. It could be seen that the decline extent of normalized flame speed as the function of initial turbulent intensity seems a geometric progression trend to the variation of normal stretch rate.

Stated thus, it could be considered that an initial turbulent flow brings enhancement in aerodynamic motion on flame-front; the enhanced relative motion promotes both the stretch effects and the wrinkling process of flame-front. On one hand, the aggravated wrinkling effects further exacerbate the unstable development uniting the role of emerging intrinsic hydrodynamic instability, as the exacerbated unstable development enlarges the contact area of flame-front to unburned mixtures; on the other hand, the enhanced stretch effects at same flame size of laminar premixed flame play a more important positive role on flame-front which '*pull*' the flame-front advance. Undergoing both the more positive effects on flame-front and the enlarged contact area of flame-front, the flame propagation speed is raised, and the increase extent is positive related to initial turbulent intensity.

## CONCLUSION

The propagation speed of wrinkled premixed flames within stoichiometric hydrogen-air mixtures has been studied under standard temperature and pressure (STP) with different initial turbulent intensities in a fan-stirred combustion vessel, the variation regulations of flame propagation speed were determined, the nexus between cellularity phenomenon and flame propagation speed was analyzed, the role of global stretch effects on flame propagation speed was also discussed, and some results and conclusion were gained as,

During the propagation process of stoichiometric hydrogen premixed flames within initial turbulent ambience,

• The flame-front could maintain stable and smooth appearance in the initial period of development (highly similar to laminar premixed flame), but such period could not be held for a long time, for obvious distortion and cells ceaselessly form. Different from laminar flames, the formation of cells is always after the distortion of flame-front, namely, ambient turbulence makes the flame-front wrinkled and subsequently promotes the formation of cells. Both first and second critical flame radii of cellularity monotonously decline with the increase of turbulent intensity, and the decline rates gradually raises.

• The global stretch rate rapidly declines in power trend and the decline rate is reduced with the increase of initial turbulent intensity, namely, turbulent intensity could bring enhancement on stretch effects. Furthermore, the increased extent of global stretch rate (compared to laminar premixed flame) monotonically rises as flame develops, namely, the positive role of turbulent flow on stretch effects not only will disappear but will continue to strengthen as flame develops. Such positive effects brought on by turbulent flow on stretch effects are achieved mainly through the channel of wrinkling flame's curvature.

• Flame propagation speed will accurately rise after a period of linear growth trend, and the onset of such phenomenon is considered relative to the appearance of cellularity phenomenon. Undergoing the effects of initial turbulent ambience, the same level of the enhancement in global stretch effects could bring larger growth of flame propagation speed under a weaker turbulent intensity, and such phenomenon becomes more obvious at a higher value of normalized global stretch rate. The enhancement of flame propagation speed is mainly attributed to the aggravated positive effects of stretch and the enlarged contact area of flame-front, and both the two factors are brought by initial turbulence on flame-front.

## ACKNOWLEDGEMENTS

This work is supported by National Natural Science Foundation of China under award 51606007, Beijing Natural Science Foundation under award 3174053, Fundamental Research Funds for the Central Universities under award 2016JBM050, and Research Foundation for Talented Scholars under award 2016RC035.

## REFERENCES

1. J.-H. Lee, D.-G. Lee, J.-I. Park and J.-Y. Kim, *Korean J. Chem. Eng.*, **27**, 187 (2010).
2. K. K. Pant, R. Jain and S. Jain, *Korean J. Chem. Eng.*, **28**, 1859 (2011).
3. D. L. Cho, H.-N. Kim, M. Lee and E. Cho, *Korean J. Chem. Eng.*, **32**, 2519 (2015).
4. Z.-Y. Sun and G.-X. Li, *Renew. Sust. Energy Rev.*, **51**, 830 (2015).
5. F. N. Pekhota, V. D. Rusanov and S. P. Malyshenko, *Int. J. Hydrogen Energy*, **23**, 967 (1998).
6. Z.-Y. Sun, F.-S. Liu, X.-H. Liu, B.-G. Sun and D.-W. Sun, *Int. J. Hydrogen Energy*, **37**, 664 (2012).
7. L. M. Das and V. Dutta, *Int. J. Hydrogen Energy*, **40**, 4280 (2015).
8. M. C. Lee, J. Yoon, S. Joo and Y. Yoon, *Int. J. Hydrogen Energy*, **40**, 11032 (2015).
9. K. Y. Foo, *Renew. Sust. Energy Rev.*, **51**, 1477 (2015).
10. M. Harada, T. Ichikawa, H. Takagi and H. Uchida, *Comp. Hydrogen Energy*, **4**, 321 (2016).
11. S. Verhelst and T. Wallner, *Prog. Energy Combust. Sci.*, **35**, 490 (2009).
12. A. Thomas, *Combust. Flame*, **65**, 291 (1986).
13. K. Liu, A. A. Burluka and C. G. W. Sheppard, *Fuel*, **107**, 202 (2013).
14. J.-H. Wang, M. Zhang, Y.-L. Xie, Z.-H. Huang, T. Kudo and H. Kobayashi, *Exp. Therm. Fluid Sci.*, **50**, 90 (2013).
15. J. Vancoillie, G. Sharpe, M. Lawes and S. Verhelst, *Fuel*, **130**, 76 (2014).
16. R. C. Aldredge, *Combust. Sci. Tech.*, **178**, 1201 (2006).
17. D. Bradley, M. Lawes and M. S. Mansour, *Combust. Flame*, **158**, 123 (2011).

18. F. Wu, A. Saha, S. Chaudhuri and C. K. Law, *Proc. Combust. Inst.*, **35**, 1501 (2015).
19. H. Wei, D. Gao, L, Zhou, J. Pan, K. Tao and Z. Pei, *Fuel*, **180**, 157 (2016).
20. Z. Wang, E. Motheau and J. Abraham, *Proc. Combust. Inst.*, **36**, 3423 (2017).
21. M. Izumikawa, T. Mitani and T. Niioka, *Combust. Flame*, **73**, 207 (1988).
22. R. C. Aldredge and B. Zuo, *Combust. Flame*, **127**, 2091 (2001).
23. O. C. Kwon, G. Rozenchan and C. K. Law, *Proc. Combust. Inst.*, **29**, 1775 (2002).
24. S. Yang, A. Saha, F. Wu and C. K. Law, *Combust. Flame*, **171**, 112 (2016).
25. Y. Xie, J. Wang, X. Cai and Z. Huang, *Int. J. Hydrogen Energy*, **41**, 18250 (2016).
26. R. Dobashi, S. Kawamura, K. Kuwana and Y. Nakayama, *Proc. Combust. Inst.*, **33**, 2295 (2011).
27. R. Keppeler and M. Pfitzner, *Combust. Theory Modell.*, **19**, 1 (2014).
28. A. N. Lipatnikov and J. Chomiak, *Prog. Energy Combust. Sci.*, **28**, 1 (2002).
29. J. F. Driscoll, *Prog. Energy Combust. Sci.*, **48**, 857 (2008).
30. J. Goulier, A. Comandini, F. Halter and N. Chaumeix, *Proc. Combust. Inst.*, **36**, 2823 (2016).
31. P. Brequigny, F. Halter and C. Mounaïm-Rousselle, *Exp. Therm. Fluid Sci.*, **73**, 33 (2016).
32. Z.-Y. Sun, F.-S. Liu, X.-C. Bao and X.-H. Liu, *Int. J. Hydrogen Energy*, **37**, 7889 (2012).
33. Z.-Y. Sun, G.-X. Li, H.-M. Li, Y. Zhai and Z.-H. Zhou, *Energies*, **7**, 4938 (2014).
34. M. Zaytsev and V. Bychkov, *Phys. Rev. E*, **66**, 026310 (2002).
35. D. Bradley, M. Lawes, K. Liu, S. Verhelst and R. Woolley, *Combust. Flame*, **149**, 162 (2007).
36. D. Bradley, M. Lawes and M. S. Mansour, *Combust. Flame*, **156**, 1462 (2009).
37. Z. Chen, *Combust. Flame*, **162**, 2442 (2015).
38. M. Faghih and Z. Chen, *Sci. Bull.*, **61**, 1296 (2016).
39. Z.-Y. Sun and G.-X. Li, *Energy*, **116**, 116 (2016).
40. D. Bradley, *Proc. R. Soc. A*, **357**, 3567 (2000).